Cellular and molecular events in the localization of diabetogenic T cells to islets of Langerhans

Boris Calderon, Javier A. Carrero, Mark J. Miller, and Emil R. Unanue[1]

Department of Pathology and Immunology, Washington University School of Medicine, St. Louis, MO 63110

Contributed by Emil R. Unanue, December 16, 2010 (sent for review November 17, 2010)

Understanding the entry of autoreactive T cells to their target organ is important in autoimmunity because this entry initiates the inflammatory process. Here, the events that lead to specific localization of diabetogenic CD4 T cells into islets of Langerhans resulting in diabetes were examined. This was evaluated in two models, one in which T cells specific for a hen-egg white lysozyme (HEL) peptide were injected into mice expressing HEL on β cells and the other using T cells in the nonobese diabetic mouse strain, which develops spontaneous diabetes. Only T cells specific for β-cell antigens localized in islets within the first hours after their injection and were found adherent to intraislet dendritic cells (DCs). DCs surrounded blood vessels with dendrites reaching into the vessels. Localization of antigen-specific T cells did not require chemokine receptor signaling but involved class II histocompatibility and intercellular adhesion molecule 1 molecules. We found no evidence for nonspecific localization of CD4 T cells into normal noninflamed islets. Thus, the anatomy of the islet of Langerhans permits the specific localization of diabetogenic T cells at a time when there is no inflammation in the islets.

T-cell migration | type 1 diabetes

The molecular basis and mechanisms involved in the spontaneous physiological migration of lymphocytes into lymph node and other sites are well understood (1–3). In contrast, the cellular events that lead lymphocytes to enter tissues bearing their cognate antigen are still to be fully identified. The site of entry of the cells, the specificity of their initial interactions, and whether there is random entry and/or retention, as well as the events that follow entry, are issues that need consideration. These events may vary depending on the anatomical features of the organ, the network of antigen-presenting cells (APCs), the state of the disease, and the controlling mechanisms of the disease, for examples. The entrance of autoreactive T cells to their target organ is particularly important because it initiates the autoimmune disease. These events have been examined mainly in the case of central nervous system autoimmunity (4). Entrance of T cells into the brain was shown, particularly following inflammation (5–7). Their retention depended on the class II MHC molecules bearing APCs (8–10). Once specific T cells were in play, they dictated the migration of nonspecific T cells (7, 9–11).

We examine here the early migratory events in autoimmune diabetes, focusing exclusively on the early time points preceding β-cell destruction. The islets of Langerhans is a relatively easy tissue to sample, wherein the target, the β cell, is well defined anatomically and the parameters of cellular migration and tissue responses can be probed with confidence. Recent studies posited a specific accumulation of diabetogenic T cells in islets several weeks after their injection (12). How diabetogenic CD4 T cells enter islets of Langerhans to initiate the diabetic process and the possible role of intraislet APCs need to be evaluated, however.

In a previous study, we confirmed that normal islets contained APCs with features of dendritic cells (DCs) (13). One important feature was their very high content of peptide–MHC complexes derived from β-cell proteins in a process unrelated to β-cell death. These DCs were highly effective in presenting β-cell antigens to diabetogenic CD4 T cells ex vivo (13–15). It is also known that the lymph nodes draining the pancreas contain APC-bearing β-cell antigens (16, 17) and are essential for the initiation of diabetes and the priming of CD4 T cells (i.e., diabetogenic CD4 T cells). Mice lacking the pancreatic nodes developed diabetes if the diabetogenic T cells were activated before transfer (18, 19), however, indicating that the pancreas is receptive to diabetogenic T cells. Here, we show that the islet DCs are in tight contact with the islet vessels, even to the point of extending their dendrites into the lumen. These DCs mediate the localization of specific CD4 diabetogenic T cells. In the companion paper in PNAS (20), we find that the specific localization initiates a number of rapid changes in gene expression and protein display in the intraislet vessels as well as in the β cell itself.

Results

Diabetogenic CD4 T Cells Specifically Localize in Islets. The experiments centered on the early stages of CD4 T-cell migration into islets preceding diabetes. We examined whether the migration and trapping of T cells were antigen-specific and depended on antigen presentation by islet cells. Our studies included two experimental systems, H-2^k mice expressing membrane hen-egg white lysozyme (HEL) in β cells under the rat insulin promoter (IP) (21, 22) and the diabetes-susceptible nonobese diabetic (NOD) mice (23). For the former, the transferred cells were from the T-cell receptor (TCR) transgenic mice 3A9, directed to a dominant peptide of HEL presented by the class II MHC molecule I-A^k; the recipients were either IP-HEL mice or mice that did not express HEL, which served as controls (B10.BR). The use of the IP-HEL mice allowed us to examine the issue of specificity by comparing localization of T cells into islets expressing or not expressing HEL. For the NOD mice, the BDC2.5 (BDC) TCR transgenic mouse was used. The BDC CD4 T cell recognizes a β-cell antigen presented by I-A^{g7} molecules (24); the recipient mice were NOD *Rag1*$^{-/-}$. The transfer of the anti-HEL CD4 T cells (3A9) into sublethally irradiated IP-HEL mice or of BDC CD4 T cells into nonirradiated NOD *Rag1*$^{-/-}$ mice caused diabetes starting several days later, depending on the number of cells transferred (25).

We took advantage of these experimental models to examine whether there is specific localization of CD4 T cells into islets of Langerhans and, if so, the mechanisms involved in such a process. Our studies examined islets of Langerhans from a few hours up to 72 h after the T-cell transfer (a critical period preceding the autoimmune reaction) at a time when T cells were not proliferating. The quantitative estimates were done only on isolated islets by examining 50–100 of them microscopically. In frozen sections of the whole pancreas, the T cells were also localized inside the islet between 1 and 12 h after transfer, but it was not possible to perform precise quantitation using tissue sections. All the experiments used recipient mice lacking lymphocytes (either sublethally irradiated or Rag1$^{-/-}$ mice); such mice developed diabetes after cell transfer in the absence of putative control mechanisms that may exist in the course of normal diabeto-

Author contributions: B.C., J.A.C., and E.R.U. designed research; B.C. performed research; M.J.M. contributed new reagents/analytic tools; B.C., J.A.C., and E.R.U. analyzed data; and B.C., J.A.C., and E.R.U. wrote the paper.

The authors declare no conflict of interest.

Freely available online through the PNAS open access option.

[1]To whom correspondence should be addressed. E-mail: unanue@pathology.wustl.edu.

This article contains supporting information online at www.pnas.org/lookup/suppl/doi:10.1073/pnas.1018973108/-/DCSupplemental.

genesis. This approach allowed us to probe the basic mechanism without superimposed events.

Activated 3A9 CD4 T cells rapidly localized to the islets of sublethally irradiated IP-HEL mice. T-cell entry was first observed at 1 h, increasing progressively with time (Fig. 1*A* and Table 1). T cells were not found in the stroma at the time of their first identification in islets (Table S1). The same number of 3A9 TCR transgenic T cells transferred into IP-HEL did not localize to the islets of IP-HEL mice. To exclude effects of sublethal irradiation, activated 3A9 T cells were transferred into nonirradiated IP-HEL mice and found to be equally distributed as seen in sublethally irradiated recipients. Activated 3A9 T cells were not detected in the islets of sublethally irradiated B10.BR mice; that is, nonspecific localization was not observed at any time point (Fig. 1*A*). In other experiments, islets from mice injected with Con A did not contain activated T cells at a time when these were abundant in the circulation. Thus, the localization of the T cells depended on their activation status as well as on the presence of their cognate antigen, HEL, in the islets.

In experiments using NOD *Rag1*$^{-/-}$ mice, activated BDC T cells localized to the pancreas shortly after their injection (Fig. 1*B* and Table 1). Unstimulated BDC T cells were not detected until 72 h and only in 20% of islets (Fig. 1*B*). Evaluation for the presence of the memory T cells in the unstimulated transfer showed that about 15–20% of the BDC clonotype CD4 T cells contained low levels of CD45RB and high levels of CD44 and leukocyte function-associated antigen-1 (LFA), which is the phenotypic characteristic of memory T cells (26). This highly indicates that a subset of the diabetogenic T cells have already encountered its antigen in the donor BDC mouse. In a control experiment, the CD4 T cells from B6.g7 either nonactivated or in vitro activated with Con A did not localize in the islets or pancreatic stroma when injected into NOD *Rag1*$^{-/-}$ mice. B6.g7 mice lack diabetogenic CD4 T cells. Activated BDC T cells did not localize to islets of NOD MHC class II-deficient [NOD,129S2(B6)-*H2-Ab1*^{tm1Gru}] mice (0%) but localized to islets of NOD MHC class II-sufficient mice (about 50% of islets contained T cells) (Fig. 1 *C* and *D*). In both the HEL and NOD systems, treatment of the diabetogenic T cells with pertussis toxin had no effect whatsoever, implying that signaling by chemokines was not involved in the localization (data shown in the companion paper, ref. 20).

The localization of BDC T cells into the islet was not related to homeostatic expansion because their transfer into immunocompetent NOD male mice also showed equal localization compared with that found in NOD *Rag1*$^{-/-}$ mice. Divisions in the activated diabetogenic T cells labeled with the dye carboxy-fluorescein diacetate succinimidyl ester (CFSE), were not found (i.e., there was no reduction in CFSE in cells that localized to the islets).

Table 1. Localization of activated transferred T cells inside islets of Langerhans

	Mean % of infiltrated islets	SD	Median no. of T cells per infiltrated islets
3A9 into	0	0	0
No transfer			
IP-HEL			
5 min	4	0	1
1 h	6	0	2
2 h	3	0	1
8 h	7	4	2
12 h	19	8.9	2
24 h	55	19.8	11
48 h	95	10.7	48
BDC into			
No transfer	0	0	0
NOD *Rag1*$^{-/-}$			
24 h	12	1.8	3
48 h	58	16.4	11
72 h	94	6.3	29

3A9 and BDC CD4 T cells were detected with their clonotype-specific antibody or anti-CD4.

Anti-Class II MHC and Anti–ICAM-1 mAbs Reduce CD4 T-Cell Localization. The specific localization of diabetogenic T cells suggested a role for antigen-specific TCR engagement of class II MHC molecules. The only cells in noninflamed islets bearing class II MHC molecules were the intraislet APCs; neither β cells nor endothelial cells were positive (13). The localization of CD4 T cells was consistently inhibited, albeit partially, by prior injection of mAb against class II MHC molecules. The reduction was specific; that is, anti–I-A^{k} but not anti–I-A^{g7} affected the localization of 3A9 T cells into IP-HEL islets, whereas the reverse was true for the entry of BDC T cells into NOD *Rag1*$^{-/-}$ islets.

Six independent experiments showed localization of 3A9 T cells after 24 h in 69% and 68% of islets in untreated mice and in mice injected with nonspecific mAb (anti–I-A^{g7}), respectively (Fig. 2 *A* and *B* and Table S2). The administration of the specific mAb (anti–I-A^{k}) partially reduced the localization to 33% of the islets (Fig. 2 *A* and *B* and Table S2), however. By 48 h, the islets were infiltrated equally and the difference in the number of T cells per islet was not statistically significant (Fig. 2*B* and Table S2). Increasing the number of injections of anti-class II MHC mAb (1 d before T-cell transfer and 1 day after) gave the same results.

The localization of BDC T cells after 48 h was affected by the administration of the mAb to I-A^{g7} but not by that of anti–I-A^{k}. In four experiments, the percentage of islets bearing CD4^{+} T cells decreased from 69% in untreated mice and 70% in mice treated with the irrelevant anti–I-A^{k} mAb to 27% in mice treated with anti–I-A^{g7} mAb (Fig. 2 *C* and *D* and Table S3). By 72 h, all groups showed the same extent of T-cell infiltration (91–99%) (Fig. 2*D* and Table S3).

The partial inhibition of CD4 T-cell entry into the islet by class II MHC mAb suggested other contributing factors, such as a role for adhesion molecules. The vessels of the islets were weakly positive for intercellular adhesion molecule 1 (ICAM-1), strongly positive for platelet endothelial cell adhesion molecule 1 (PECAM-1), and negative for vascular cell adhesion molecule-1 and P-selectin (13). Administering a blocking mAb to PECAM-1 did not affect T-cell localization into islets; however, a blocking mAb to ICAM-1 partially reduced the localization of activated 3A9 T cells transferred into IP-HEL mice to 41% at 24 h from control rat IgG of 71% (Fig. 3 *A* and *B*) and to 78% by 48 h from control rat IgG of 98% (median of 17 and 33 T cells per infiltrated islet, respectively). Flow cytometry analysis of the T cells showed that 97% expressed LFA-1, the ligand of ICAM-1. When a combination of anti-class II MHC and anti–ICAM-1 was administered, the partial inhibition of localization was not enhanced (Fig. 3 *A* and *B*).

Activated BDC T cells were transferred into sublethally irradiated NOD.ICAM-1$^{+/+}$ or NOD.ICAM-1$^{-/-}$ mice (27) that received either anti–I-A^{k} or anti–I-A^{g7} mAb (Fig. 3 *C* and *D*). Localization was slightly reduced in the ICAM-1$^{-/-}$ mice compared with that found in the control islets at 48 h after T-cell transfer. The best effects were found when the NOD.ICAM-1$^{-/-}$ mice were treated with anti–I-A^{g7} mAb. NOD.ICAM-1$^{-/-}$ mice treated with anti–I-A^{g7} mAb contained BDC T cells in 26% of islets compared with 59% in NOD.ICAM-1$^{-/-}$ mice treated with anti–I-A^{k} mAb or NOD.ICAM-1$^{+/+}$ mice treated with anti–I-A^{g7} mAb (Fig. 3 *C* and *D*).

In sum, T cells localized specifically to islets containing their antigen and the localization was partially inhibited by antibodies to class II MHC molecules and ICAM-1. The partial inhibition could well be explained by the very rapid amplification reactions that take place in the islet as soon as there is T-cell entry, an issue discussed in the companion paper (20). Not surprisingly, because the reduction in T-cell entry was only partial, injecting anti-class II MHC mAbs did not affect diabetes development. Diabetes was delayed by 3–5 d when activated BDC T cells were transferred into sublethally irradiated NOD.ICAM-1$^{-/-}$ mice treated with the anti–I-A^{g7} mAb (100% of control NOD.ICAM-1$^{+/+}$ mice plus anti-IA^{k} mAb

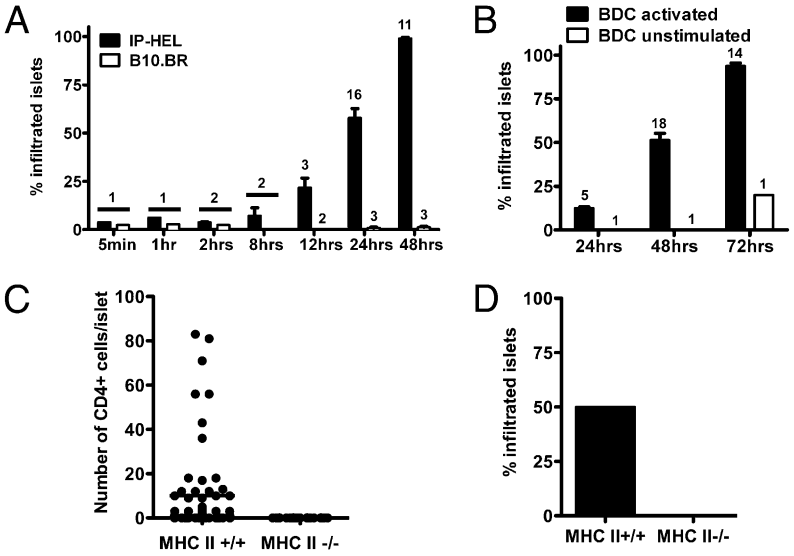

Fig. 1. Localization of CD4 T cells to islets containing their antigen and MHC class II requirement. (*A*) Pooled results showing localization of activated 3A9 T cells into sublethally irradiated B10.BR and IP-HEL recipients at different times. Numbers of experiments are indicated on each bar. (*B*) Transfer of activated or unstimulated BDC T cells into NOD *Rag1*$^{-/-}$ recipients, analyzed at different time points. Numbers of experiments are indicated on each bar. (*C*) Localization of CD4 T cells into MHC class II-sufficient or -deficient mice. Activated BDC T cells were transferred into sublethally irradiated 8-wk-old NOD male mice (MHC II$^{+/+}$) or MHC class II$^{-/-}$ deficient mice. The graph shows the number of infiltrated CD4 T cells per islet at 48 h after cell transfer. (*D*) Percentage of infiltrated islets from previous experiments (*C*). Data are represented as the mean (±SEM).

treatment developed diabetes at day 9 after cell transfer, whereas NOD.ICAM-1$^{-/-}$ mice treated with the anti–I-A^{g7} developed diabetes by day 12 and 100% incidence by day 15 after cell transfer).

Islet DCs Have Direct Access to the Lumen of the Vessel and Are Found in Contact with Specific Infiltrating CD4 T Cells. Islets were analyzed by two-photon microscopy mostly in the HEL system, wherein B10.BR mice always served as controls. In 3D reconstruction analysis, about 50% of 3A9 T cells in islets from IP-HEL mice were in tight contact with DCs, with an average contact time of 7.4 min (Fig. 4). By the last points of observation (10–15 min), 39% of the T cell-DC interactions were still stable. The prolonged T cell-DC interaction of 3A9 cells is compatible with the finding that the cognate antigen for the former is present in the islet DCs. [In lymph nodes, the T cell-DC interaction in the absence of antigen had a mean duration of 3.4 min and did not extend for more than 10 min. In the presence of antigen, contact durations ranged from 8 to 20 min, with some lasting for more than 1 h (28).]

DCs in explanted islets moved closely around blood vessels while having an adhesion point in the vessel wall, extending and retracting their dendrites. (So as not to use mAbs, which could affect DC mobility, these experiments used C57BL/6 mice expressing YFP under the *Cd11c* promoter. Blood vessels were stained for PECAM-1). The area of physical contact was evident as fluorescence colocalization (Fig. 5*A*). Analysis of captured 3D images (1.5-μm z-steps) or by confocal microscopy allowed the visualization of DCs. The majority were in direct contact with the blood vessels with their dendrites embedded within the vessel. In about one-third of them, dendrites extended into the lumen of the vessel (i.e., "periscope" function) through the endothelium (Fig. 5 *B* and *C*).

To examine whether the islet DCs next to blood vessels were instrumental in localization, we used anti-class II mAb-coated fluorescent beads (anti–I-A^{k} or anti–I-A^{g7}) administered via tail vein injection into B10.BR, B6.g7, or NOD mice. At 30–60 min after fluorescent bead injection, isolated islets from B10.BR recipient mice (I-A^{k} background) showed ∼90% of the islets containing the fluorescent beads coated with anti–class II I-A^{k} mAb, whereas B6.g7 and NOD mice (I-A^{g7} background) contained ∼14% and ∼10%, respectively (from three independent experiments). The number of beads localizing specifically was much higher, as noted in Fig. 5*D*. Parallel results were obtained when anti–I-A^{g7} mAb-coated fluorescent beads were transferred into B6.g7, NOD, and B10.BR recipients (∼63%, ∼60%, and ∼30%, respectively) (Fig. 5*D*, taken from three independent experiments). Importantly, localization of the anti–class II mAb- coated beads was restricted to the vessels, and most were found at the vessel wall next to a DC (Fig. 5*E*).

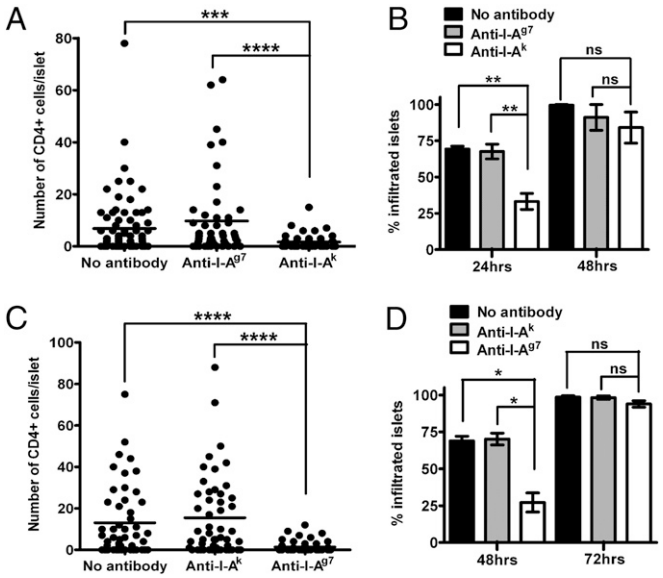

Fig. 2. Localization of CD4 T cells to islets during partial inhibition by anti-class II MHC mAb. (*A*) T-cell distribution in islets 24 h after transfer of activated 3A9 T cells into IP-HEL mice treated as indicated, 1 d before cell transfer. The graph shows a representative experiment from a total of six, and each dot represents an islet. (*B*) Percentage of T cell-infiltrated islets at 24 and 48 h in IP-HEL mice treated as in *A*. Results are pooled from six and four experiments at 24 and 48 h, respectively. (*C*) T-cell distribution in islets 48 h after transfer of activated BDC T cells into NOD *Rag1*$^{-/-}$ mice treated as indicated. The graph shows a representative experiment from four experiments. (*D*) Percentage of T cell-infiltrated islets at 48 and 72 h in mice treated as in *C*. Results are pooled from four experiments. Data are represented as the mean (±SEM). $P \geq 0.05$ [not significant (ns)]; *$P < 0.05$; **$P < 0.01$; ***$P < 0.001$; ****$P < 0.0001$.

Discussion

Using a procedure in which the migration of CD4 T cells to islets of Langerhans was determined within the first hours after their injection, we proved the specificity of their localization and examined the mechanisms of such a process: Localization of diabetogenic CD4 T cells was a relatively fast event that depended on the state of activation of the diabetogenic T cells. The islet DC network bearing the peptide–MHC complexes from β cells guided the entrance in a process partially dependent on class II

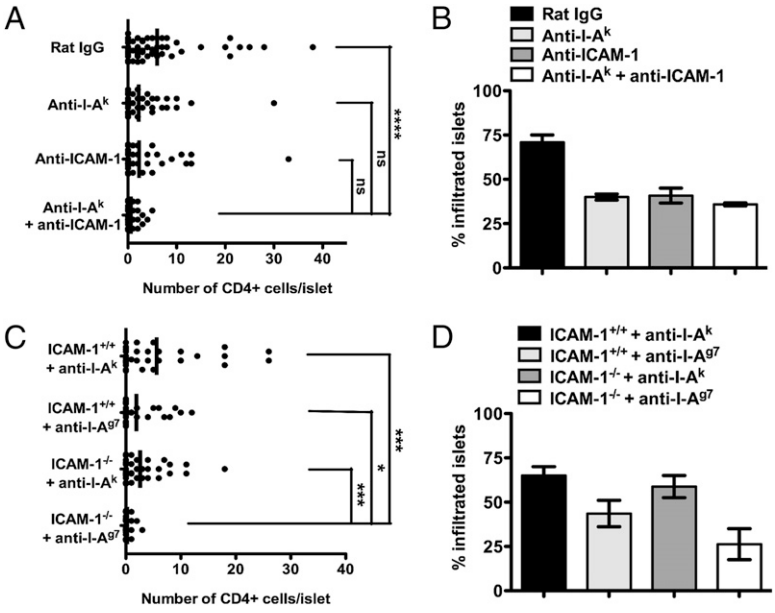

Fig. 3. Partial inhibition of T-cell localization by anti-class II MHC and ICAM-1 mAb. (*A*) T-cell distribution in islets 24 h after transfer of activated 3A9 T cells into IP-HEL mice treated with a single mAb or a combination of both, 1 d before cell transfer. The graph shows a representative experiment from a total of two experiments. (*B*) Percentage of infiltrated islets from the previous experiment (*A*), showing the compiled data from two experiments. (*C*) T-cell distribution in islets 48 h after the transfer of activated BDC T cells into sublethally irradiated NOD.ICAM-1$^{+/+}$ and NOD.ICAM-1$^{-/-}$ mice treated with a single anti-class II blocking mAb as indicated, 1 d before cell transfer. The graph shows a representative experiment from a total of two experiments. (*D*) Percentage of infiltrated islets from the previous experiment (*C*), showing the compiled data from two experiments at 48 h. Data are represented as the mean (±SEM). $P \geq 0.05$ [not significant (ns)]; $^*P < 0.05$; $^{***}P < 0.001$; $^{****}P < 0.0001$.

MHC and ICAM-1 molecules. Thus, the anatomical features of islets allow for the specific localization of diabetogenic CD4 T cells, the step preceding the inflammatory response that leads to beta cell demise.

The islet DCs were central in the localization of diabetogenic T cells. Over 90% of intraislet DCs were heavily charged with peptide–MHC complexes involving HEL peptides or peptides derived from β cells in a constitutive process that involved neither an obvious death cell program nor prior inflammation (13, 14). Most of the islet DCs were in intimate contact with the vessels, and, surprisingly, many extruded their fine ramifications into the vessel wall, most likely through the endothelial fenestrae. Precedents of DC dendrites penetrating epithelial and vascular beds were described in the intestine as a mechanism of immune surveillance allowing the DCs to sample lumen bacteria through the epithelium (29–31). Airway intraepithelial DCs have been shown to extend projections into the airway lumen (32), and it has recently been reported that aortic resident DCs can capture blood antigen by periscoping and then present it to circulating leukocytes that can induce vessel wall inflammation (33). The finding that circulating beads bearing anti-class II antibodies localized preferentially to islets bearing the correct class II specificity and always at the vessel wall argues strongly for a role of the DC in fostering the localization of the diabetogenic T cells. It is important to note that the circulation of the islets is sluggish and intermittent. Only a few vessels are opened at one time (34, 35), a feature conducive to initial interactions in the vessel lumen. One could posit that T cells enter islets at random and then either escape back into circulation or are retained, depending on whether they engage the antigen-bearing DC. This last process would require a very fast turnover of this putative cycle of entrance and exit of T cells, which we have failed to substantiate. A scenario of random nonspecific entry and trapping of only those T cells with specific TCRs was described in the experimental autoimmune encephalomyelitis models (7, 10, 36, 37), however.

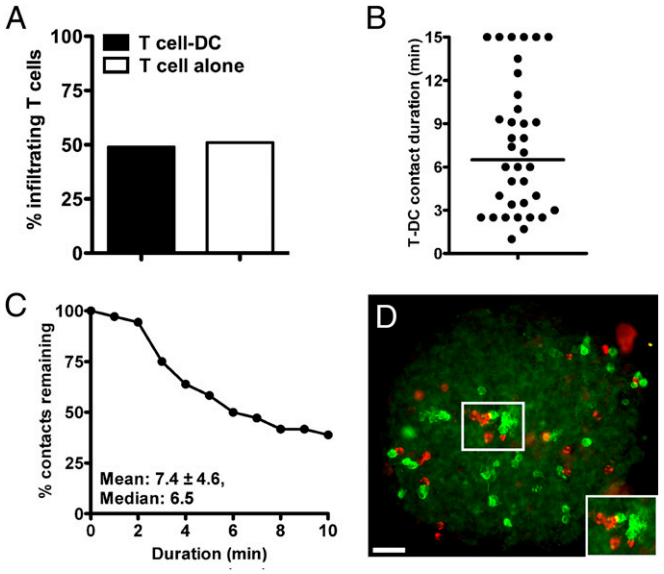

Fig. 4. T cell-DC interaction in islets by two-photon microscopy and immunofluorescence. (*A*) Live isolated islet analysis evaluating percentage of 3A9 T cells found in contact with islet DCs at 24 h after cell transfer. T cell-DC contacts were obtained from a total of 20 examined islets from two independent experiments. 3A9 T cells were detected with anti-CD4 mAb, and DCs were detected with anti-CD11c mAb. (*B*) Plot shows T cell-DC contact durations of 3A9 (CFSE-labeled) T cells at 24 h after cell transfer in IP-HEL mice. Contact durations were obtained from 10- to 15-min time-lapse movies from two experiments. (*C*) Analysis showing percentage of T cell-DC remaining contact for any given duration. (*D*) Infiltrated islet at 24 h after activated T-cell transfer showing 3A9 T cells (red) and CD11c cells (green). (*Inset*) Micrograph showing contact of T cells with CD11c cells (yellow merged color). (Scale bar, 50 μm.)

Finally, the evidence points to the fact that the localization of T cells was directly into islets from the circulation without a stop in the periislet areas. The question is raised because there is initial infiltration of leukocytes surrounding the islets without apparent effect on β cells in the very early stages of diabetogenesis; this is followed by an aggressive phase with inflammation (22, 38, 39). Whether the periislet lymphocytes initiated this aggressive stage or it resulted from activated T cells entering from blood is not known.

We previously showed that most of the intraislet DCs, over 90%, were heavily charged with peptide–MHC complexes involving HEL peptides or peptides derived from β cells in a constitutive process that involved neither an obvious death cell program nor prior inflammation (13, 14). Our interpretation is that some of the islet DCs with their high content of peptide–MHC complexes from β cells migrate from islets into the stroma and then through the lymphatics to finally drain into the peripancreatic lymph node, where sensitization of T cells takes place (16, 17). There is compelling evidence that the draining pancreatic lymph node is the site

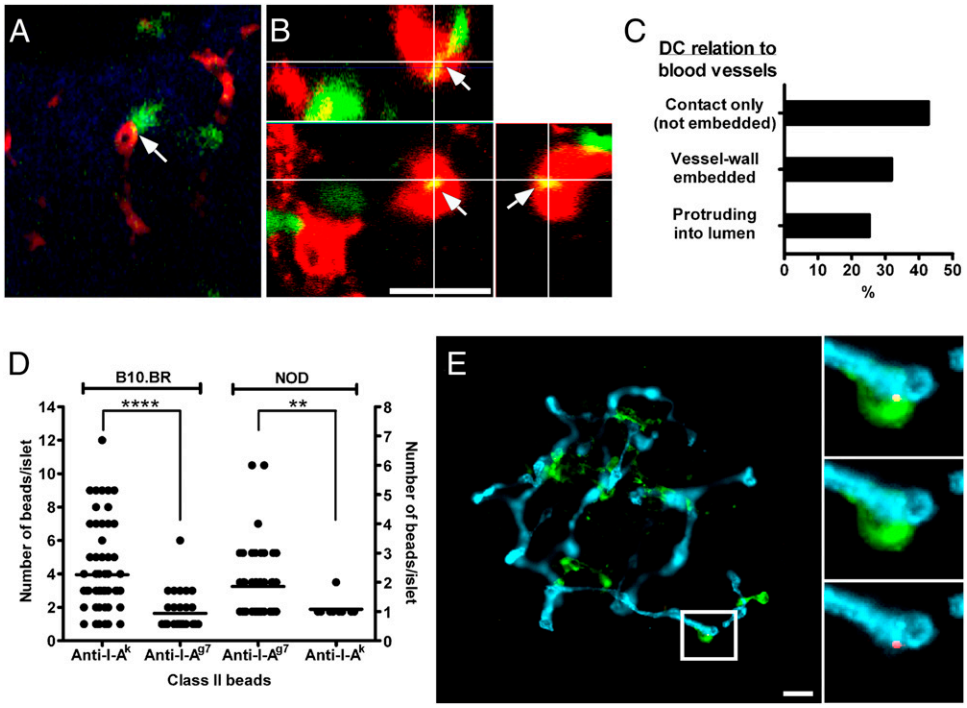

Fig. 5. Analysis of islet DCs in direct contact with blood vessels. (*A*) Two-photon microscopic analysis of a representative islet of C57BL/6 mice expressing YFP under the CD11c promoter (CD11c-YFP, shown in green) and endothelia stained with PECAM-1 (red). Reconstruction from a single stack (1-μm thickness). The arrow shows a DC in apposition to the vessel and dendrite, reaching into the lumen (yellow merging color). (*B*) 3D reconstruction by confocal microscopy of an islet from CD11c-YFP mice with vessels stained in red (PECAM-1) and CD11c-YFP (green). (*Lower Left*) Projection along the *z* axis (top view) from a stack of 30 optical sections (0.5-μm increments). (*Upper Right*) *z–x* and *z–y* reconstructions (side view) of same image stack (indicated as white lines). The image shows a DC dendrite inside the vessel (yellow merged color indicated by arrows). (*C*) Percentages of DCs contacting the vessel wall (not embedded), dendrites in the vessel wall, or DCs protruding into the lumen ($n = 108$). Data were obtained from 17 different visualized fields from two experiments. (*D*) Quantitative analysis of anti-class II mAb fluorescent bead (anti–I-A^k or anti–I-A^{g7}) localization. Each dot represents a single islet. The left and right *y* axes show the number of anti-class II beads per islet in B10.BR and NOD mice, respectively, representing compiled data from three independent experiments. $^{**}P < 0.01$; $^{****}P < 0.0001$. (*E*) Localization of anti-class II–coated beads by immunofluorescence in islets of B10.BR mice previously injected i.v. with beads coated with anti–I-A^k. Islet DCs are shown in green (CD11c), blood vessels are shown in blue (PECAM-1), and fluorescent beads are shown in red. (*Insets*) Micrograph showing a representative islet DC in contact with a bead inside the lumen of the vessel. Bead and PECAM-1 (*Bottom Right*); CD11c and PECAM-1 (*Middle Right*); bead, CD11c, and PECAM-1 (*Top Right*). (Scale bar, 20 μm.)

of recruitment and activation of the T cells but that activated diabetogenic T cells can cause diabetes in mice lacking lymph nodes (18, 19). These findings are supported by the present experiments in which the localization of diabetogenic CD4 T cells required a brief activation ex vivo, whereas the localization of the same but nonactivated cells was limited, perhaps requiring further priming in vivo. At this time, we do not have an explanation, but a likely one may be the level of adhesion molecules, such as LFA-1, and/or TCR expression.

A previous report by Lennon et al. (12) analyzed the infiltrating CD4 T cells but at 4.5–6.5 wk after injection of their transduced bone marrow. This long time interval did not allow the examination of entry mechanisms, while making the time of evaluation more complex because of (*i*) the unknown diabetogenic status of the mice and (*ii*) the proliferative advantage of specific T cells that entered the islets and encountered their specific antigen over the nonspecific clones that never encountered their antigen. In that report, TCR specificity for islet antigens was the sole key factor dictating entry (12). With regard to the CD8 T cells, the migration into islets was examined by others (40), particularly by Chervonsky and colleagues (41). With one clone, they showed notable differences from the diabetogenic CD4 T cells. The CD8 T cells required MHC class I expression attributed to the endothelium and a chemokine response (pertussis toxin treatment abolished specific CD8$^+$ T-cell entry) as well as IFN-γ for extravasation of the T cell into the islet milieu (41, 42). Both sets of T cells (CD4 and CD8) share some common pathways in the pathogenesis of the disease.

Understanding how various cells localize to the islets, interact, or influence each other; the factors that contribute to their localization/retention; and the signals that are triggered in the islet milieu will all need to be placed in the perspective of the normal diabetogenic process. Our studies provide a baseline to examine these variables. The development of therapeutics that can modulate the islet localization of diabetogenic T cells may provide the means to control this autoimmune disease.

Materials and Methods

Mice. B10.BR mice, B10.BR.RIP-mHEL (IP-HEL) mice (21, 22), C57BL/6 mice expressing YFP under the CD11c promoter (CD11c-YFP) (43), NOD mice, BDC TCR transgenic mice on the NOD background, B6.g7 mice, and 3A9 mice were bred at our facility. NOD on the *Rag1*$^{-/-}$ (NOD *Rag1*$^{-/-}$) [NOD.129S7(B6)-*Rag1*^{tm1Mom}/J], NOD.ICAM-1$^{-/-}$ [NOD.129S4(B6)-*Icam1*^{tm1Jcgr}/J], male NOD.IFN-γR$^{-/-}$ [NOD.129S1(B6)-*Ifngr2*^{tm1Pbro}/DvsJ], and NOD MHC class II-deficient [NOD,129S2(B6)-*H2*-Ab1^{tm1gru}] mice were obtained from the Jackson Laboratory. The institutional animal care committee approved these studies.

T-Cell Transfers. T cells were first activated in vitro before i.v. injection (25). BDC splenocytes were cultured with a mimotope peptide (1 μM) and 3A9 and B10.BR splenocytes in 100 nM HEL or Con A (2 μg/mL) (Sigma–Aldrich), respectively. CD4 T cells were isolated by negative selection using MACS Cell Separation Columns (Miltenyi Biotec). Mice received a dose of 1–2 × 10^7 T cells administered i.v. IP-HEL, B10.BR, NOD, and NOD.ICAM-1$^{-/-}$ mice received a sublethal dose of irradiation (6.5 Gy) before T-cell injection. In some experiments, CD4 T cells were labeled with Vybrant CFDA SE, CellTracker Red CMTPX, or CellTracker Blue CMAC (Invitrogen). Diabetes incidence was followed as previously described (25).

Antibody Treatments. Mice received mAb administered i.p. 1 d before T-cell transfer: 500 μg of anti–I-A^{g7} (clone AG2.42.7), anti–I-A^k (clone 40F), anti–

PECAM-1 (clone 2B8, kindly provided by Steven Bogen, Boston University School of Medicine, Boston, MA) (44), and 400 μg of anti–ICAM-1 (clone BE29G1). Isotype control rat IgG (Sigma–Aldrich) antibodies were used.

Anti-Class II Fluorescent Beads. SPHERO streptavidin-coated fluorescent particles (0.4–0.6 μm, Nile Red; Spherotech, Inc.) were conjugated with biotinylated anti–I-A^k (clone 40F) or anti–I-A^{g7} (clone AG2.42.7) mAb for 1 h following the manufacturer's binding capacity specifications. Conjugated beads were washed twice in PBS by centrifugation (2,000 × *g*). Anti-class II beads were administered i.v. (3×10^6 beads in a 200-μL volume of PBS), and islets were isolated at 30–60 min after injection.

Islet Isolation and Handling. Islet isolation, staining for immunofluorescence analysis by standard microscopy with epiillumination, and confocal and two-photon microscopy were performed as previously described (13, 14). Infiltrating T cells were detected by means of their clonotype-specific mAb, anti-CD4 mAb, Vybrant CFDA SE, CellTracker Red CMTPX, or CellTracker Blue CMAC (Invitrogen). A summary of antibodies is listed in Table S4.

Statistical Analysis. The Mann–Whitney *U* test was used to determine the level of significant differences between samples and was plotted using GraphPad Prism 5 (GraphPad Software, Inc.). The following *P* values were detected: $^{****}P < 0.0001$, $^{***}P < 0.001$, $^{**}P < 0.01$, $^{*}P < 0.05$, and $P \geq 0.05$ (not significant). Median numbers of T cells per infiltrated islets in all experiments were obtained by including only islets containing infiltrating T cells.

ACKNOWLEDGMENTS. We thank Katherine Frederick, Jeremy Herzog, Patrice Bittner, and Shirley Petzold for technical assistance, and members of the E.R.U. laboratory, particularly Roger Belizaire and Jim Mohan, for helpful discussions. This work was supported by National Institutes of Health Grants AI024742, DK058177, and P60DK20579; Juvenile Diabetes Research Foundation Grant JDRF 1-2007-731; and the Kilo Diabetes and Vascular Research Foundation.

1. Gallatin M, et al. (1986) Lymphocyte homing receptors. *Cell* 44:673–680.
2. Bromley SK, Mempel TR, Luster AD (2008) Orchestrating the orchestrators: Chemokines in control of T cell traffic. *Nat Immunol* 9:970–980.
3. Denucci CC, Mitchell JS, Shimizu Y (2009) Integrin function in T-cell homing to lymphoid and nonlymphoid sites: Getting there and staying there. *Crit Rev Immunol* 29:87–109.
4. Krishnamoorthy G, Wekerle H (2009) EAE: An immunologist's magic eye. *Eur J Immunol* 39:2031–2035.
5. Baron JL, Madri JA, Ruddle NH, Hashim G, Janeway CA, Jr. (1993) Surface expression of alpha 4 integrin by CD4 T cells is required for their entry into brain parenchyma. *J Exp Med* 177:57–68.
6. Katz-Levy Y, et al. (1999) Endogenous presentation of self myelin epitopes by CNS-resident APCs in Theiler's virus-infected mice. *J Clin Invest* 104:599–610.
7. Flügel A, et al. (2001) Migratory activity and functional changes of green fluorescent effector cells before and during experimental autoimmune encephalomyelitis. *Immunity* 14:547–560.
8. Greter M, et al. (2005) Dendritic cells permit immune invasion of the CNS in an animal model of multiple sclerosis. *Nat Med* 11:328–334.
9. Kawakami N, et al. (2005) Live imaging of effector cell trafficking and autoantigen recognition within the unfolding autoimmune encephalomyelitis lesion. *J Exp Med* 201:1805–1814.
10. Archambault AS, Sim J, Gimenez MA, Russell JH (2005) Defining antigen-dependent stages of T cell migration from the blood to the central nervous system parenchyma. *Eur J Immunol* 35:1076–1085.
11. Goverman J (2009) Autoimmune T cell responses in the central nervous system. *Nat Rev Immunol* 9:393–407.
12. Lennon GP, et al. (2009) T cell islet accumulation in type 1 diabetes is a tightly regulated, cell-autonomous event. *Immunity* 31:643–653.
13. Calderon B, Suri A, Miller MJ, Unanue ER (2008) Dendritic cells in islets of Langerhans constitutively present β cell-derived peptides bound to their class II MHC molecules. *Proc Natl Acad Sci USA* 105:6121–6126.
14. Mohan JF, et al. (2010) Unique autoreactive T cells recognize insulin peptides generated within the islets of Langerhans in autoimmune diabetes. *Nat Immunol* 11:350–354.
15. Levisetti MG, Lewis DM, Suri A, Unanue ER (2008) Weak proinsulin peptide-major histocompatibility complexes are targeted in autoimmune diabetes in mice. *Diabetes* 57:1852–1860.
16. Höglund P, et al. (1999) Initiation of autoimmune diabetes by developmentally regulated presentation of islet cell antigens in the pancreatic lymph nodes. *J Exp Med* 189:331–339.
17. Sarukhan A, Lechner O, von Boehmer H (1999) Autoimmune insulitis and diabetes in the absence of antigen-specific contact between T cells and islet beta-cells. *Eur J Immunol* 29:3410–3416.
18. Gagnerault MC, Luan JJ, Lotton C, Lepault F (2002) Pancreatic lymph nodes are required for priming of β cell reactive T cells in NOD mice. *J Exp Med* 196:369–377.
19. Levisetti MG, Suri A, Frederick K, Unanue ER (2004) Absence of lymph nodes in NOD mice treated with lymphotoxin-β receptor immunoglobulin protects from diabetes. *Diabetes* 53:3115–3119.
20. Calderon B, Carrero JA, Miller MJ, Unanue ER (2011) Entry of diabetogenic T cells into islets induces changes that lead to amplification of the cellular response. *Proc Natl Acad Sci USA* 108:1567–1572.
21. Akkaraju S, et al. (1997) A range of CD4 T cell tolerance: Partial inactivation to organ-specific antigen allows nondestructive thyroiditis or insulitis. *Immunity* 7:255–271.
22. Byersdorfer CA, Schweitzer GG, Unanue ER (2005) Diabetes is predicted by the β cell level of autoantigen. *J Immunol* 175:4347–4354.
23. Tisch R, McDevitt H (1996) Insulin-dependent diabetes mellitus. *Cell* 85:291–297.
24. Katz JD, Wang B, Haskins K, Benoist C, Mathis D (1993) Following a diabetogenic T cell from genesis through pathogenesis. *Cell* 74:1089–1100.
25. Calderon B, Suri A, Unanue ER (2006) In CD4+ T-cell-induced diabetes, macrophages are the final effector cells that mediate islet β-cell killing: Studies from an acute model. *Am J Pathol* 169:2137–2147.
26. Jenkins MK, et al. (2001) In vivo activation of antigen-specific CD4 T cells. *Annu Rev Immunol* 19:23–45.
27. Martin S, et al. (2001) Dominant role of intercellular adhesion molecule-1 in the pathogenesis of autoimmune diabetes in non-obese diabetic mice. *J Autoimmun* 17:109–117.
28. Miller MJ, Safrina O, Parker I, Cahalan MD (2004) Imaging the single cell dynamics of CD4+ T cell activation by dendritic cells in lymph nodes. *J Exp Med* 200:847–856.
29. Rescigno M, et al. (2001) Dendritic cells express tight junction proteins and penetrate gut epithelial monolayers to sample bacteria. *Nat Immunol* 2:361–367.
30. Chieppa M, Rescigno M, Huang AY, Germain RN (2006) Dynamic imaging of dendritic cell extension into the small bowel lumen in response to epithelial cell TLR engagement. *J Exp Med* 203:2841–2852.
31. Hapfelmeier S, et al. (2008) Microbe sampling by mucosal dendritic cells is a discrete, MyD88-independent step in DeltainvG S. Typhimurium colitis. *J Exp Med* 205:437–450.
32. Jahnsen FL, et al. (2006) Accelerated antigen sampling and transport by airway mucosal dendritic cells following inhalation of a bacterial stimulus. *J Immunol* 177:5861–5867.
33. Choi JH, et al. (2009) Identification of antigen-presenting dendritic cells in mouse aorta and cardiac valves. *J Exp Med* 206:497–505.
34. Wayland H (1997) Microcirculation in pancreatic function. *Microsc Res Tech* 37:418–433.
35. Carlsson PO, Källskog O, Bodin B, Andersson A, Jansson L (2002) Multiple injections of coloured microspheres for islet blood flow measurements in anaesthetised rats: Influence of microsphere size. *Ups J Med Sci* 107:111–120.
36. Hickey WF, Hsu BL, Kimura H (1991) T-lymphocyte entry into the central nervous system. *J Neurosci Res* 28:254–260.
37. Ransohoff RM, Kivisäkk P, Kidd G (2003) Three or more routes for leukocyte migration into the central nervous system. *Nat Rev Immunol* 3:569–581.
38. Katz J, Benoist C, Mathis D (1993) Major histocompatibility complex class I molecules are required for the development of insulitis in non-obese diabetic mice. *Eur J Immunol* 23:3358–3360.
39. Matsumoto M, et al. (1993) Transfer of autoimmune diabetes from diabetic NOD mice to NOD athymic nude mice: The roles of T cell subsets in the pathogenesis. *Cell Immunol* 148:189–197.
40. Pang S, et al. (2009) CD8(+) T cells specific for β cells encounter their cognate antigens in the islets of NOD mice. *Eur J Immunol* 39:2716–2724.
41. Savinov AY, Wong FS, Chervonsky AV (2001) IFN-γ affects homing of diabetogenic T cells. *J Immunol* 167:6637–6643.
42. Savinov AY, Wong FS, Stonebraker AC, Chervonsky AV (2003) Presentation of antigen by endothelial cells and chemoattraction are required for homing of insulin-specific CD8+ T cells. *J Exp Med* 197:643–656.
43. Lindquist RL, et al. (2004) Visualizing dendritic cell networks in vivo. *Nat Immunol* 5:1243–1250.
44. Bogen S, Pak J, Garifallou M, Deng X, Muller WA (1994) Monoclonal antibody to murine PECAM-1 (CD31) blocks acute inflammation in vivo. *J Exp Med* 179:1059–1064.